COMMUNICATION

ChemComm
www.rsc.org/chemcomm

# Nanostructured silicon surfaces *via* nanoporous alumina

**Matthias Kruse, Steffen Franzka and Günter Schmid***
*Institut für Anorganische Chemie, Universität Essen, Universitätsstr. 5-7, 45117 Essen, Germany.*
*E-mail: guenter.schmid@uni-essen.de; Fax: +49 201 1832401; Tel: +49 201 1834195*

*Received (in Cambridge, UK) 2nd February 2003, Accepted 17th April 2003*
*First published as an Advance Article on the web 13th May 2003*

**Nanostructured silicon surfaces are generated using nanoporous alumina membranes as stamps to imprint PMMA films on silicon, followed by reactive ion etching (RIE).**

Generating nano- and microstructured surfaces has become an important field in nanoscience, nanotechnology, and microtechnology for several reasons. These surfaces are characterized by novel properties as compared to planar surfaces. This concerns optical properties as well as different interactions towards other materials. For instance, wettability behavior can dramatically vary, depending on the surface structure. Appropriately structured surfaces improve the reflection properties of glass-like materials. Due to practical consequences of those interesting properties, various processes have been developed to generate micro- and nanostructured surfaces. Most important contributions in this respect came from Whitesides *et al*.[1–3] They use imprinting techniques to structure various materials by masks that were generated before by lithographic methods. Usually, these processes result in structures in the micro regime, due to the limitations of the tools used. The coverage of surfaces by nanoparticles is another route to nanostructure surfaces, however, it is rather difficult to produce well defined architectures. Recently, we described a method to decorate smooth surfaces with metal nanoparticles, using electrospray or pneumatic spray techniques.[4] Also recently, we reported an imprinting process that allows structuring of surfaces with structure units ranging from a few nanometers up to 200 nm, using nanoporous alumina as imprinting masks.[5] Metals and polymers have been imprinted successfully using this technique. Here we report a process to create nanostructured silicon surfaces by indirect means, since silicon can not be imprinted directly, owing to its brittleness. Herein, we report for the first time the use of nanoporous alumina to form nanostructured silicon surfaces. This is accomplished by imprinting spincoated PMMA films on silicon surfaces with nanoporous alumina to form a nanostructured PMMA surface. These features are then transferred into the silicon substrate by established RIE techniques.[6–10]

The process is schematically shown in Fig. 1, which in the following is described in detail.

A thin film of PMMA is spincoated onto the silicon surface (Fig. 1, A1). The thickness is measured with an Atomic Force Microscope (AFM) to be 70 ± 5 nm. PMMA as an imprint medium in nanotechnology is well known.[11,12] PMMA, being thermoplastic, is heated above its glass transition temperature (105 °C) so that it can be easily structured by the mask (A2). After cooling down to 80 °C the mask is removed and a negative form of the mask is obtained on the PMMA surface.

The mask to imprint PMMA consists of nanoporous alumina (Fig. 1, A2). It is routinely available by anodization of aluminium surfaces. The formation mechanism of those well developed pore systems has variously been studied and described in the literature.[13–18] One of the numerous advantages of this material is the ability to control its pore width and pore length over wide size ranges from a few up to several hundred nm. The width depends directly on the anodization voltage, the length on the anodization time. Since the pores are all running parallel through the oxide layer and perpendicular to the surface, this surface is characterized by $10^9$–$10^{11}$ pores cm$^{-1}$, depending on the pore size. Large extended hexagonal structures can only be observed under very distinct experimental conditions. Fig. 2 shows an AFM image of a routinely available alumina membrane.

As a typical example of our process,[†] we describe the generation and use of 50 nm pores. In order to have a good quality imprinting tool, we used aluminium discs of 30 mm in diameter and 6 mm thick. In order to planarize the aluminium surface the discs are mechanically polished by a half-automated polishing system. After careful polishing, a pre-anodization step was carried out in oxalic acid at 40 V and 0 °C for 30 minutes. The resulting aluminium oxide layer is then removed using chromic acid, as it is known that such a pre-anodization improves the quality of the final pore structure.[14,15] The anodization is carried out for 60 minutes under the same conditions as the pre-anodization step. This process gives rise to an imprinting material of high quality. Anodization at 40 V results in pores of *ca.* 50 nm diameter. It was found that it is essential to use very pure aluminium (99.999%) for this process

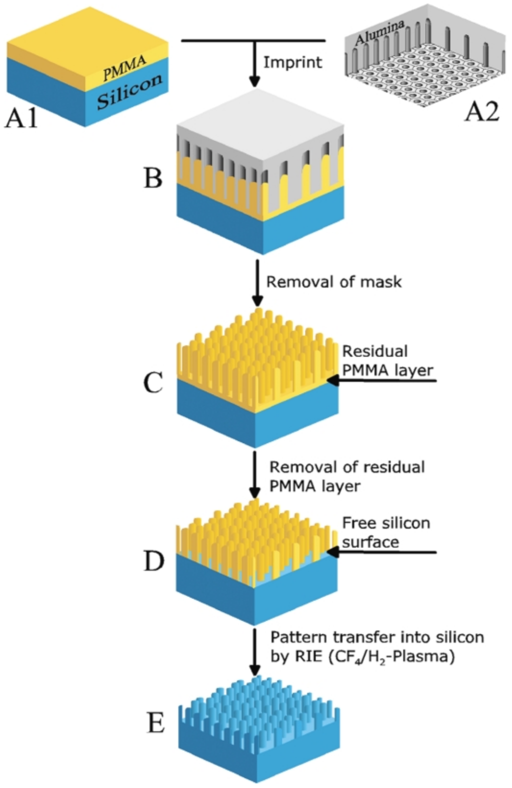

**Fig. 1** Sketch illustrating the generation of nanostructured silicon surfaces. A thin PMMA film on silicon is generated by spincoating (A1). A mask of nanoporous alumina (A2) is imprinted into the PMMA film (B), resulting in PMMA pillars (C). A thin PMMA film remaining on the silicon surface between the pillars is then removed by means of an oxygen plasma (D). This is followed by an RIE step to transfer the pattern into the silicon substrate (E).

DOI: 10.1039/b301340e

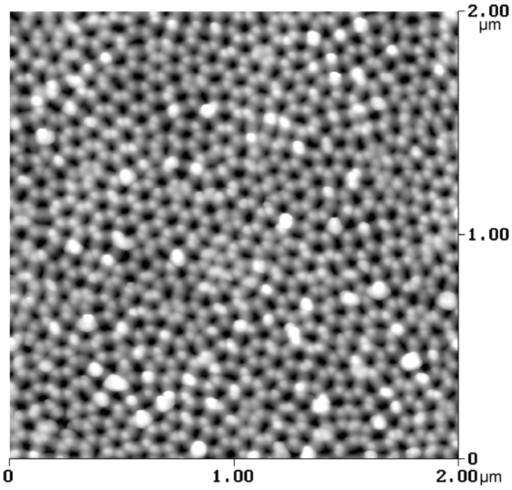

**Fig. 2** AFM image of a routinely generated nanoporous alumina mask with pores of ≈50 nm in diameter, $z$ range = 50 nm.

because, if the purity is not high enough, inclusions of various alloy particles will stick out of the surface after polishing the aluminium. These inclusions will prevent conformal contact of the alumina stamp with the PMMA layer, leading to non-uniform pattern transfer.

The imprint process takes place under pressure and at elevated temperatures (Fig. 1B). The temperature to imprint PMMA layers should be above its glass transition temperature. That guarantees that the PMMA can move into the pores. Optimum results were obtained in the temperature range of 140 to 160 °C and an applied pressure of $3.0 \times 10^7$–$3.6 \times 10^7$ Pa. If the pressure is too low, insufficient transfer of the pore structure into PMMA takes place. On the other hand, if the pressure is too high, the wafer will be destroyed. Under optimum conditions, PMMA flows into the pores, creeps along the inner pore walls and fills them, resulting in pillar structures. The flow process ends when a specific height of the pillars is reached. This height is determined by the applied pressure, the imprinting temperature and initial thickness of the PMMA layer.

After imprinting the temperature is lowered to 80 °C and then the mask is removed (Fig. 1C). It is essential that the PMMA be cooled down below its glass temperature in order to avoid peeling of the PMMA layer by the mask. An AFM image of a PMMA layer imprinted using our process is shown in Fig. 3.

It can clearly be seen that the hexagonal pore structure is transferred by the imprinting process from the nanoporous alumina mask into the PMMA layer, resulting in PMMA pillars. AFM investigation gave a height of 160 ± 30 nm and about 50 nm in diameter, corresponding to the stamp. Considering the AFM tip geometry, the height is difficult to determine and can only be measured at defects.

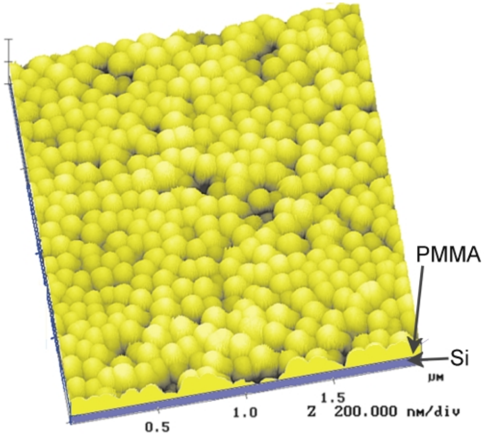

**Fig. 3** AFM image of a PMMA layer imprinted by a mask of nanoporous alumina.

As mentioned above, the flow of the PMMA into the pore structure stops at a specific height of the pillars, meaning that the PMMA layer is not imprinted down to the wafer surface, but there remains a residual layer between the pillars. The thickness of this thin PMMA film was measured at defects by AFM and was found to be <20 nm. To realize an optimal pattern transfer into the silicon, this layer has to be removed by applying an anisotropic oxygen plasma (Fig. 1D). As found in previous experiments, the etching rate of PMMA under the conditions described in the experimental part is about 80 nm $\text{min}^{-1}$. After an etching time of 10 to 15 s, the residual PMMA layer between the pillars is completely removed, as can clearly be seen in Fig. 4.

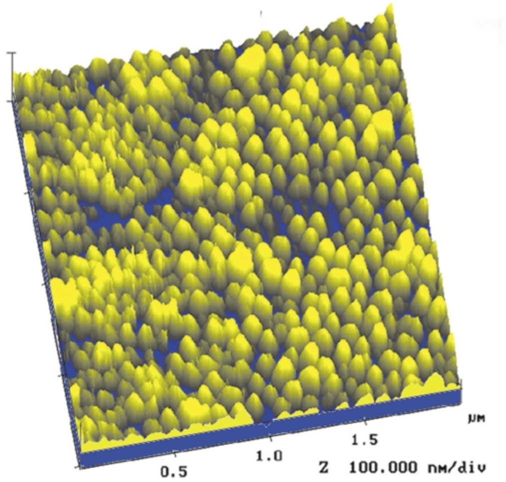

**Fig. 4** PMMA pillar structure after treating with oxygen plasma (yellow = PMMA, blue = silicon surface).

After oxygen plasma treatment the pillars (yellow in Fig. 4) reach down to the silicon surface (blue in Fig. 4). However, the oxygen plasma not only removes residual PMMA but also attacks the PMMA pillars. So, the height of the pillars decreases during the etching process from 160 ± 30 nm to 80 ± 20 nm, while their base diameter stays constant. This means that the etching process has to be as short as possible.

The final step involves the transfer of the PMMA pillar structure into the silicon surface. (Fig. 1E). This is done by RIE, which is a conventional dry etching process routinely used in the production of microsystems. It stands out as an etching process with high anisotropy, high selectivity and high etching rates. As etching gases we used $CF_4$ for etching the silicon and $H_2$ for removing impurities, especially traces of polymers *etc.* After a final, cleaning oxygen plasma treatment, immediately after RIE, the silicon wafers were removed from the etching chamber and investigated by AFM (Fig. 5).

As can be seen, the PMMA pillar structure is successfully transferred by RIE into the silicon, resulting in a nanostructured silicon surface. The height of the pillars was found 50 ± 15 nm, whereas the thickness <25 nm, considering the AFM tip geometry. The silicon pillars do not have identical heights and furthermore, the pillars are etched as well, rounding off their tops. This means that the PMMA pillars are also removed during etching the silicon. Due to the fact that the PMMA pillars do not have identical heights, some of them are removed quicker than others so that the etching gases can also attack the subjacent silicon pillars, resulting in the structures as shown in Fig. 5. Even reduced etching times (down to 30 s) give the same results, *i.e.* PMMA is etched much faster than silicon. From experience it can be deduced that not only RIE, but also the oxygen plasma, attacks the silicon. Volatile $SiO_x$ species may be formed, resulting in further etching and thinning of the pillars.

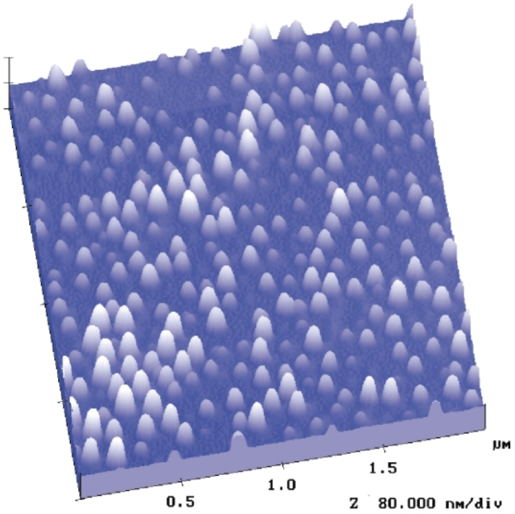

**Fig. 5** Nanostructured silicon surface after RIE and oxygen plasma treatment.

From the SEM image in Fig. 6 it can be seen that the nanopillars are spread over a wide range on the silicon surface. In fact it can be assumed that the whole wafer surface is covered in the same way as is shown in Fig. 6.

In conclusion it can be stated that nanoporous alumina membranes have for the first time been used to nanostructure silicon wafer surfaces. The special advantage of this easily available material is the variability of the pore size and herewith of the final structure on the silicon surface. On the way *via* an imprinted PMMA film on silicon, this nanostructure is transferred into the wafer surface by a reactive ion etching process (RIE) with $CF_4$ and $H_2$. The etching process has to be improved so that silicon nanopillars of the same height will be formed. Those nanostructured silicon surfaces might be applicable on various fields, for instance field emission or luminescing surfaces. One further goal in our research is the use of those silicon pillars as contacts for individual metal or semiconductor quantum dots. To reach this goal, thinner silicon pillars would be favorable. Indeed, we also succeeded in generating $< 20$ nm pillars by using alumina masks with 25 nm pores.

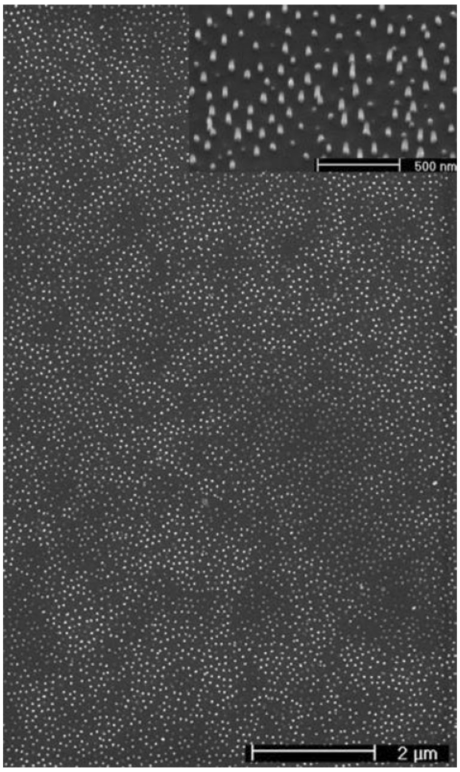

**Fig. 6** SEM image of a larger cutout of a nanostructured silicon surface.

We gratefully acknowledge financial support of this work by the Deutsche Forschungsgemeinschaft and the Fonds der Chemischen Industrie, Frankfurt.

## Notes and references

† The generation of nanoporous alumina is described elsewhere.[11–16] In this case, the following specific conditions were applied: aluminium disks (99.999%) of 30 mm in diameter and 6 mm thickness were mechanically ground and polished by a half-automatic polishing system (Rotopol 31, Rotoforce 4). Then, the disks were pre-anodized in oxalic acid (0.3 wt%) at 0 °C and a voltage of 40 V for 30 min. The achieved porous layer was removed by chromic acid (4.8 wt%) at 80 °C in the course of 30 min. This first anodization was performed to improve the ordering degree of the final pores. After careful rinsing with pure water, the final anodization took place under the same conditions, but over 60 min. Silicon wafers (orientation (111), $10 \times 10$ mm$^2$, As doped, 0.003 Ω cm) were covered by thin PMMA films (950 K, 2% solution in chlorobenzene) by spincoating (Spincoater Model 6700, Speciality Coating Systems, Inc.). The thickness of the PMMA films was found to be 70 ± 5 nm (AFM). These films were then imprinted by the oxide coated aluminium disk under various pressures ($1 \times 10^7$ Pa–$1 \times 10^8$ Pa) and temperatures between 140 and 160 °C for 30 min. The pressure was maintained during cooling down to about 100 °C. Then, the pressure was released, cooling down was continued to about 80 °C and the mask was removed. The whole imprint process, including cooling down, takes about 15 min. After the imprint process, there remains a thin film of PMMA that is not imprinted. To remove this residual PMMA layer from the surface of the wafer, an anisotropic oxygen plasma with the following conditions was applied: gas flow = 60 sccm, pressure = 3.0 Pa, power = 24 W, bias voltage = 400 V, time = 10 s, water cooled substrate. Thereafter, reactive ion etching (RIE) in a $CH_4$–$H_2$ plasma followed in order to transfer the pattern into the silicon. The $CF_4$ gas flow was 30 sccm and that of $H_2$ 6 sccm at 3.5 Pa and a Bias voltage of 400 V. The sample was water cooled and the etching time was 120 s. To remove the PMMA residues, an oxygen plasma treatment at 3.0 Pa with a gas flow of 60 sccm and a Bias voltage of 400 V over 300 s followed. The obtained structures were characterized by AFM (Nanoscope IIIa, Tapping Mode DI) and by SEM (XL30 SFEG, Philips).

1 X.-M. Zhao, Y. Xia and G. M. Whitesides, *J. Mater. Chem.*, 1997, **7**, 1069.
2 Y. Xia, J. A. Rogers, K. E. Paul and G. M. Whitesides, *Chem. Rev.*, 1999, **99**, 1823.
3 B. Xu, F. Arias and G. M. Whitesides, *Adv. Mater.*, 1999, **11**, 492.
4 F. Schulz, S. Franzka and G. Schmid, *Adv. Funct. Mater.*, 2002, **12**, 532.
5 T. Sawitowski, S. Franzka, M. Levering, N. Beyer and G. Schmid, *Adv. Funct. Mater.*, 2001, **11**, 169.
6 S. Y. Chou, P. R. Krauss and P. J. Renstrom, *Appl. Phys. Lett.*, 1995, **21**, 3114.
7 S. Y. Chou, P. R. Krauss and P. J. Renstrom, *Science*, 1996, **272**, 85.
8 B. Heidari, I. Maximov, E.-L. Sarwe and L. Montelius, *J. Vac. Sci. Technol. B*, 1999, **17**, 2961.
9 S. Y. Chou, P. R. Krauss, W. Zhang, L. Guo and L. Zhuang, *J. Vac. Sci. Technol. B*, 1997, **15**, 2897.
10 F. Gottschalch, T. Hoffmann, C. M. Sotomayor Torres, H. Schulz and H.-C. Scheer, *Solid-State Electron.*, 1999, **43**, 1079.
11 H.-C. Scheer, H. Schulz, T. Hoffmann and C. M. Sotomayor Torres, *J. Vac. Sci. Technol. B*, 1998, **16**, 3917.
12 H. Schift, R. W. Jaszewski, C. David and J. Gobrecht, *Microelectron. Eng.*, 1999, **46**, 121.
13 J. P. O′Sullivan and G. C. Wood, *Proc. R. Soc. London, Ser. A*, 1970, **317**, 511.
14 G. E. Thompson, *Thin Solid Films*, 1997, **297**, 192.
15 H. Masuda and K. Fukuda, *Science*, 1995, **268**, 1466.
16 H. Masuda and M. Satoh, *Jpn. J. Appl. Phys.*, 1996, **35**, L126.
17 A. P. Li, F. Müller, A. Birner, K. Nielsch and U. Gösele, *J. Vac. Sci. Technol. A*, 1999, **17**(4), 1428.
18 G. Schmid, *J. Mater. Chem.*, 2002, **12**, 1231.